Optica Applicata, Vol. XLIV, No. 1, 2014
DOI: 10.5277/oa140105

Transmission characteristics of ^{85}Rb and ^{87}Rb laser-induced dichroism atomic filters at 795 nm

PENG YU-FENG*, ZHANG WEN-JIN

College of Physics and Electronic Engineering, Henan Normal University, Xinxiang, Henan 453007, China

*Corresponding author: yufengp@sina.com

The transmission characteristics for ^{85}Rb and ^{87}Rb laser-induced dichroism atomic filters operating on rubidium D_1 lines (795 nm) transitions are analyzed. By means of semiclassical density matrix equations of motion, a three-level model for the transmission characteristics of the ground state laser-induced dichroism atomic filter is presented. Calculative results show that this filter, using two counterpropagating pump and probe beams, can obtain higher transmission, narrower bandwidth and larger tuning capability than that using two copropagating pump and probe beams; with the aid of counterpropagating pump, the ^{85}Rb ground state laser-induced dichroism atomic filter can be more effective to achieve higher peak transmission (>34%) and larger tunability (>1 GHz) than the ^{87}Rb ground state laser-induced dichroism atomic filter in the same operation parameters. This result may be helpful for improving peak transmission (14.6%) of Rb ground state laser-induced dichroism atomic filter reported (CERÈ A. *et al.*, Opt. Lett. **34**(7), 2009, pp. 1012–1014).

Keywords: atomic filter, optical anisotropy, narrowband, rubidium.

1. Introduction

Narrowband atomic optical filters play an important role in atmospheric [1] and underwater laser communication, free-space quantum-key distribution (QKD) [2], lidar systems [3] because of high transmission, narrow bandwidth, fast response, large field of view, and high noise rejecting capacity. A narrow band atomic filter can be realized by using the Faraday effect where a longitudinal magnetic field induces a circular birefringence in the medium. A Faraday filter exploiting birefringence was first introduced and demonstrated by ÖHMAN (1956) [4]. The theory behind Faraday anomalous dispersion optical filters (FADOFs) had been discussed previously by YEH (1982) [5]; it was improved by YIN and SHAY (1991) [6] to include the hyperfine effect. The first experimental demonstration of a FADOF was given by DICK and SHAY (1991) [7]. Then, different experiments were completed based on both ground state transitions (Na [8, 9], K [10, 11], Rb [7, 12] and Cs [13]) and excited state transitions (K [14], Rb [15]). Most of Faraday optical filters operate in a resonance line

wing, only HU *et al.* [8], CHEN *et al*. [9], ZHANG *et al*. [10] showed FADOFs operating in a line center. However, due to being subjected to a large Doppler effect, all of FADOFs have a larger bandwidth (for example, Na 2 GHz [8], K 1.5 GHz [10], Rb 1 GHz [7], Cs 0.7 GHz [13]) compared with the laser-induced dichroism atomic line filters (LIDALFs) [16–19] which can easily obtain a sub-Doppler bandwidth via a narrow-linewidth pump beam.

The laser-induced dichroism atomic line filter based on velocity-selective optical pumping was first described and demonstrated by TURNER *et al*. (2002) [16]. The filter, operating on the K $4P_{3/2} \rightarrow 6S_{1/2}$ excited state transition, achieved a sub-Doppler bandwidth (170 MHz) at a peak transmittance of 9.5%. In 2009, CERÈ *et al*. [18] demonstrated experimentally another LIDALF based on ground state transition in rubidium. It should be noted that although this ground state LIDALF achieved an ultra-narrow bandwidth of 80 MHz, its peak transmission was only 14.6%, which is much less than that of the conventional ground state FADOFs.

It is well-known that in a ground state FADOF any velocity class of atoms in the vapor may interact with the probe light and then participate in filtering process, so the bandwidth is Doppler limited but the transmission is very high. Unlike the ground state FADOF, a narrow-linewidth pump beam will excite only a narrow velocity class of atoms to involve in filtering process in a ground state LIDALF, potentially allowing for a sub-Doppler bandwidth. However, it limits the filter's transmission efficiency simultaneously.

In this paper, we present a three-level model for the transmission characteristics of the ground state LIDALF based on velocity-selective optical-pumping-induced dichroism, and analyze the influences of pump scheme (*i.e.*, the pump is copropagating or counterpropagating with the probe), pump intensity, pump detuning, cell temperature and cell length on transmission characteristics. It is found that the ^{85}Rb ground state LIDALF can achieve better transmission property than the ^{87}Rb ground state LIDALF in the same working conditions, which may be helpful for improving peak transmission of Rb ground state LIDALF in [18].

2. Theoretical model

In this work, we chose a closed Λ-type three-level system in ^{87}Rb atoms to show the principle of a ground state LIDALF, and the schematic diagram of the relevant energy levels is shown in Fig. 1. A σ^+ polarized beam (795 nm) drives $5S_{1/2}$ $F = 2$ to $5P_{1/2}$ $F' = 1$ transition in the pumping process while a linearly polarized beam (795 nm) probes the $5S_{1/2}$ $F = 2$ $m_F = +2$ to $5P_{1/2}$ $F' = 1$ or 2 $m'_F = +1$ transition. The selective optical-pumping process leads to a movement of population from the $5S_{1/2}$ $F = 2$ $m_F = -2, -1, 0$ to $5P_{1/2}$ $F' = 1$ magnetic sublevels. Due to atomic spontaneous emission, the population will finally accumulate on $5S_{1/2}$ $F = 2$ $m_F = +1, +2$ ground states. If the probe light is far from resonant with the $5S_{1/2}$ $F = 2$ $m_F = +2 \rightarrow 5P_{1/2}$ $F' = 1$ or 2

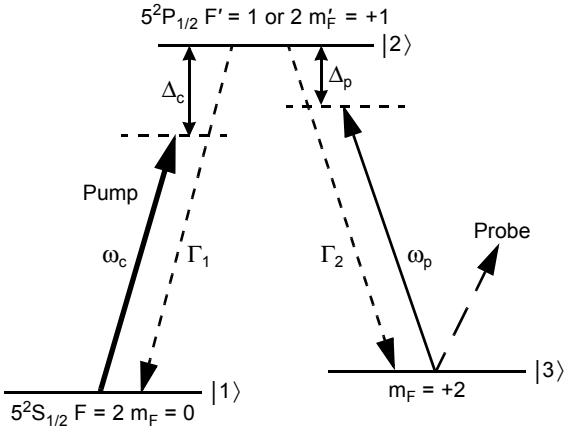

Fig. 1. The ^{87}Rb three-level Λ system. For ^{85}Rb atoms, the levels $|1\rangle$, $|2\rangle$ and $|3\rangle$ correspond to the states $5S_{1/2}$ $F = 3$ $m_F = +1$, $5P_{1/2}$ $F' = 2$ or 3 $m_F' = +2$ and $5S_{1/2}$ $F = 3$ $m_F = +3$, respectively.

$m_F' = +1$ transition, the vapor neither absorbs nor retards either component, so the unchanged polarization is blocked by the crossed polarizer. For resonant light, the σ^+ component is not absorbed or retarded, as selection rules for electric-dipole transitions forbid that. The σ^- component interacts with the vapor and is absorbed and retarded. The result is that the medium exhibits an anisotropy experienced by the linearly polarized probe field. The optical anisotropy consists of circular dichroism and birefringence, which displays differences in the absorption coefficient and the refractive index between σ^+ and σ^- circularly polarized probe components, respectively. The effect of these differences on a linearly polarized beam of probe, which may be considered to be a superposition of two equal-amplitude right and left circularly polarized beams, is the rotation of its plane of polarization. Because of this rotation, the linearly polarized probe beam can partly pass though the crossed polarizers. This is the operation mechanism of a ground state LIDALF.

In the model, the atoms are treated in quantum mechanism and the laser field is described as a classical traveling wave. In the interaction picture, with the electric-dipole and the rotating-wave approximations, the atom–laser interaction Hamiltonian can be written as

$$H_I = -\frac{\hbar}{2}\begin{bmatrix} 0 & \Omega_c & 0 \\ \Omega_c & -2\Delta_c & \Omega_p \\ 0 & \Omega_p & -2(\Delta_c - \Delta_p) \end{bmatrix} \tag{1}$$

Here Δ_c and Δ_p are the detunings of the pump and probe laser frequencies ω_c and ω_p from the corresponding atomic transitions; Ω_c and Ω_p are the Rabi frequencies of

the pump laser and probe laser. For simplicity, we take the Rabi frequencies as real. According to the Liouville equation

$$\frac{\partial \rho}{\partial t} = \frac{1}{i\hbar}[H_I, \rho] - \frac{1}{2}(\Gamma\rho + \rho\Gamma) \tag{2}$$

the semiclassical density-matrix equations of motion of the three-level system can be expressed as:

$$\dot{\rho}_{11} = \Gamma_1 \rho_{22} + \frac{i\Omega_c(\rho_{21} - \rho_{12})}{2} \tag{3a}$$

$$\dot{\rho}_{22} = -(\Gamma_1 + \Gamma_2)\rho_{22} + \frac{i\Omega_c(\rho_{12} - \rho_{21})}{2} + \frac{i\Omega_p(\rho_{32} - \rho_{23})}{2} \tag{3b}$$

$$\dot{\rho}_{33} = \Gamma_2 \rho_{22} + \frac{i\Omega_p(\rho_{23} - \rho_{32})}{2} \tag{3c}$$

$$\dot{\rho}_{21} = -(i\Delta_c + \gamma)\rho_{21} + \frac{i\Omega_c(\rho_{11} - \rho_{22})}{2} + \frac{i\Omega_p\rho_{31}}{2} \tag{3d}$$

$$\dot{\rho}_{23} = -(i\Delta_p + \gamma)\rho_{23} + \frac{i\Omega_p(\rho_{33} - \rho_{22})}{2} + \frac{i\Omega_c\rho_{13}}{2} \tag{3e}$$

$$\dot{\rho}_{31} = -\left[i(\Delta_c - \Delta_p) + \Gamma_3\right]\rho_{31} + \frac{i\Omega_p\rho_{21}}{2} - \frac{i\Omega_c\rho_{32}}{2} \tag{3f}$$

where $\gamma = (\Gamma_1 + \Gamma_2 + \Gamma_3)/2$; Γ_1 and Γ_2 are the spontaneous decay rates of the excited state $|2\rangle$ to the ground states $|1\rangle$ and $|3\rangle$, respectively; Γ_3 is the nonradiative decay rate between two ground states.

Since the atomic optical filter is used to detect a weak optical signal, we can treat the probe field as a perturbation and disregard the influence of the probe beam on the population. Therefore, at steady state, the Equations (3) yields

$$\rho_{23} = \frac{i\Omega_p\left\{4(i\Delta_c - \gamma)(\rho_{33} - \rho_{22})\left[i(\Delta_p - \Delta_c) + \Gamma_3\right] + \Omega_c^2(\rho_{11} - \rho_{22})\right\}}{2(i\Delta_c - \gamma)\left\{4(i\Delta_p + \gamma)\left[i(\Delta_p - \Delta_c) + \Gamma_3\right] + \Omega_c^2\right\}} \tag{4}$$

For the probe we have [20]

$$\mathbf{P}(z, t) = \frac{1}{2}\varepsilon_0\chi_- E_-(z, t)\hat{e}_- \exp\left[i(k_p z - \omega_p t)\right] + \text{c.c.} = \tag{5}$$

$$= N(\mu_{23}\rho_{23}\hat{e}_- + \text{c.c.})$$

The complex susceptibility χ_- of the σ^- probe transition then can be written as

$$\chi_- = \frac{2\mu_{23}^2 N\rho_{23}}{\hbar\varepsilon_0\Omega_p} \tag{6}$$

Here $\hbar$ is the Plank constant divided by 2π, ε_0 is the permittivity of vacuum, μ_{23} is the transition electronic dipole moment between states $|2\rangle$ and $|3\rangle$, and N is the number density of ^{85}Rb or ^{87}Rb atoms, given by

$$N = \xi N_0 \tag{7}$$

where ξ is the natural abundance of ^{85}Rb or ^{87}Rb atoms, and N_0 is the total Rb atomic number density, given by [21]

$$\log(N_0) = -\frac{4529.6}{T} - 3.991\log(T) + 0.00059\,T + 34.8325 \tag{8}$$

The above derivation ignores Doppler broadening. We consider the pumping laser and probe laser passing through a Doppler-broadened atomic cell in the same (opposite) direction. An atom moving towards the probe beam with velocity v is affected by the probe frequency detuning upshifted to $\Delta_p + \omega_p v/c$ and the frequency detuning of the pumping beam upshifted (downshifted) to $\Delta_c + \omega_c v/c$ ($\Delta_c - \omega_c v/c$). Considering that atoms are in classical thermal equilibrium with the one-dimensional Maxwellian velocity distribution of $N(v)\mathrm{d}v = N_0\exp(-v^2/u^2)/(u\sqrt{\pi})\mathrm{d}v$, the final value of χ_- is obtained by integrating over the atomic velocity v,

$$\chi_- = \frac{2\mu_{23}^2 N}{\sqrt{\pi}\,u\hbar\varepsilon_0\Omega_p}\int_{-\infty}^{+\infty}\rho_{23}\exp(-v^2/u^2)\mathrm{d}v \tag{9}$$

Here u is the most probable velocity and is defined as $u = (2k_BT/M)^{1/2}$, where k_B is the Boltzmann constant, T is the cell temperature and M is the mass of the atom.

The transmission coefficient of the ground state LIDALF is described as [5]

$$\mathrm{Tr} = \frac{1}{2}\exp(-\overline{\alpha}L)\Big[\cosh(\Delta\alpha L) - \cos(2\rho L)\Big] \tag{10}$$

where L is the atomic cell length; $\overline{\alpha}$, $\Delta\alpha$ and ρ are the mean absorption coefficient, circular dichroism, and rotatory power, respectively. They can be written as:

$$\overline{\alpha} = \frac{1}{2}(\alpha_+ + \alpha_-) = \frac{\omega_p}{2c}\mathrm{Im}(\chi_+ + \chi_-) \tag{11a}$$

$$\Delta\alpha = \frac{1}{2}(\alpha_+ - \alpha_-) = \frac{\omega_p}{2c}\mathrm{Im}(\chi_+ - \chi_-) \tag{11b}$$

$$\rho = \frac{\omega_p}{2c}(n_+ - n_-) = \frac{\omega_p}{4c}\mathrm{Re}(\chi_+ - \chi_-) \tag{11c}$$

3. Results and discussion

According to the hyperfine transmission model of Rb ground state LIDALF, when the pump is counterpropagating with the probe, and the pump field with an intensity of 40 mW/cm^2 is on resonance with the ^{87}Rb $5S_{1/2}$ $F = 2 \rightarrow 5P_{1/2}$ $F' = 1$ transition, the absorption coefficient and transmission of a Rb ground state LIDALF *vs.* the probe detuning from resonance with ^{87}Rb $5S_{1/2}$ $F = 2$ $m_F = +2 \rightarrow 5P_{1/2}$ $F' = 1$ or 2 $m'_F = +1$ transition are shown in Figs. 2**a** and 2**b**, respectively. It is noteworthy that there is no transmission peak of ^{85}Rb atoms displayed in Fig. 2**b**. That is because when the pump laser is tuned to the ^{87}Rb $5S_{1/2}$ $F = 2 \rightarrow 5P_{1/2}$ $F' = 1$ transition, due to velocity-selective optical pumping, only ^{87}Rb atoms within the resonant velocity group are efficiently pumped, participating in the filtering process, while ^{85}Rb atoms experience little pumping effect, keeping away from the filtering process. In the theoretical simulation, the filter, which may be referred to as the ^{87}Rb ground state LIDALF, shows a peak transmission of 16.8% with a bandwidth (full width at half maximum, FWHM) of 80 MHz. This result is in a good agreement with the experimental observation carried out by CERÈ *et al*. [18]. In the model, the Fresnel losses of the optical devices are ignored, and the depolarization effect of the probe beam passing through the medium is negligible. This is why the theoretical transmission is more than that of the experimental measurement.

The peak transmission and bandwidth of the ^{87}Rb ground state LIDALF as a function of the pump intensity are shown in Fig. 3 where the pump and probe beams are counterpropagating and in Fig. 4 where the pump and probe beams are copropagating. It is clearly shown in Figs. 3 and 4 that the peak transmission increases rapidly with

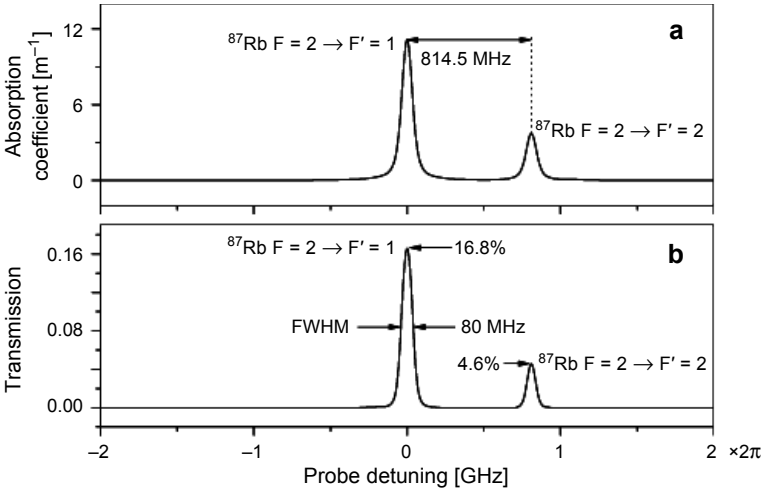

Fig. 2. Absorption coefficient (**a**), and transmission (**b**) as a function of the probe detuning. Both transmission peaks are corresponding to ^{87}Rb $5S_{1/2}$ $F = 2$ $m_F = +2 \rightarrow 5P_{1/2}$ $F' = 1$ or 2 $m'_F = +1$ probe transitions from left to right, respectively. The pump field is on resonance with ^{87}Rb $5S_{1/2}$ $F = 2 \rightarrow$ $\rightarrow 5P_{1/2}$ $F' = 1$ transition; $I_{\text{pump}} = 40$ mW/cm^2, $T = 338$ K and $L = 15$ cm.

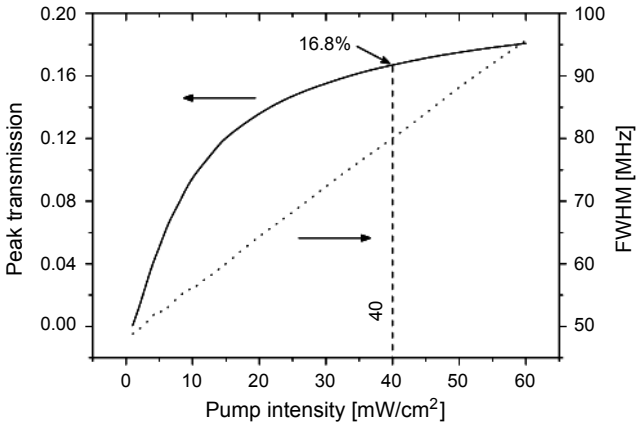

Fig. 3. Peak transmission (solid curve) and FWHM (dotted line) as a function of the pump intensity at 338 K when pump and probe beams are counterpropagating. The pump beam is resonant with ^{87}Rb $5S_{1/2}$ $F = 2 \rightarrow 5P_{1/2}$ $F' = 1$ transition. The probe beam is on resonance with ^{87}Rb $5S_{1/2}$ $F = 2$ $m_F = +2 \rightarrow$ $\rightarrow 5P_{1/2}$ $F' = 1$ $m'_F = +1$ transition; $L = 15$ cm.

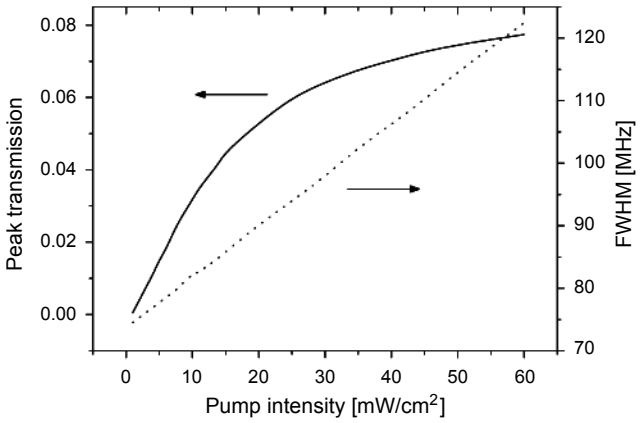

Fig. 4. Peak transmission (solid curve) and FWHM (dotted line) as a function of the pump intensity at 338 K when pump and probe beams are copropagating. Other working parameters are the same as Fig. 3.

increasing pump intensity over a certain pump intensity range, and above this range, the peak transmission is relatively insensitive to the pump intensity. The peak transmission increases with the increment of pump intensity in both ranges; however, the physical mechanism behind them is different. In lower pump intensity, the pump transition is unsaturated. The increment of pump intensity can populate more atoms to the $5S_{1/2}$ $F = 2$ $m_F = +2$ state, causing the increase in transmission. In higher pump intensity, the pump transition becomes saturated, so the population of the $5S_{1/2}$ $F = 2$ $m_F = +2$ state should not significantly increase; but higher pump intensity can pump a broader velocity group of atoms resulting from power broadening into the $5S_{1/2}$ $F = 2$ $m_F = +2$ state, leading to the increase in transmission. Through comparing Figs. 3

and 4, we find that in the same operation conditions, the filter adopting two counterpropagating pump and probe beams can achieve higher peak transmission and narrower bandwidth than that using two copropagating pump and probe beams due to the elimination of Doppler effect.

The dependence of peak transmission and peak shift of the ^{87}Rb ground state LIDALF on pump detuning is shown in Fig. 5 when the pump is counterpropagating

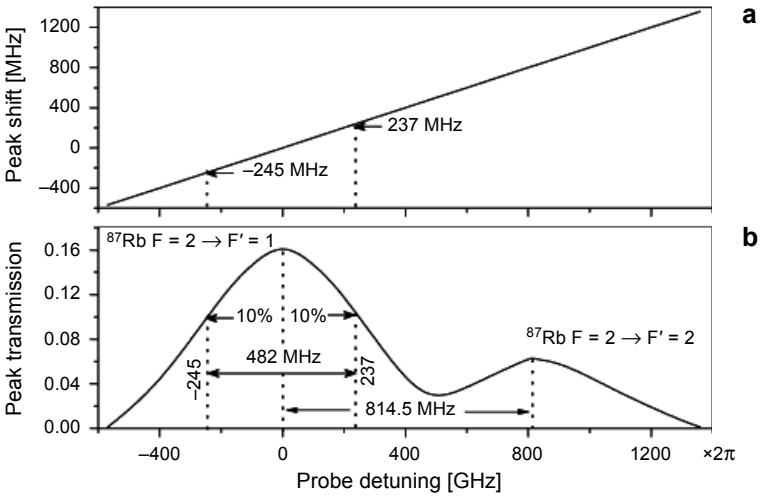

Fig. 5. The dependence of peak shift (**a**) and peak transmission (**b**) on pump detuning from the ^{87}Rb $5S_{1/2}$ $F = 2 \rightarrow 5P_{1/2}$ $F' = 1$ transition when the pump is counterpropagating with the probe; $I_{\text{pump}} =$ $= 40$ mW/cm^2, $T = 338$ K and $L = 15$ cm.

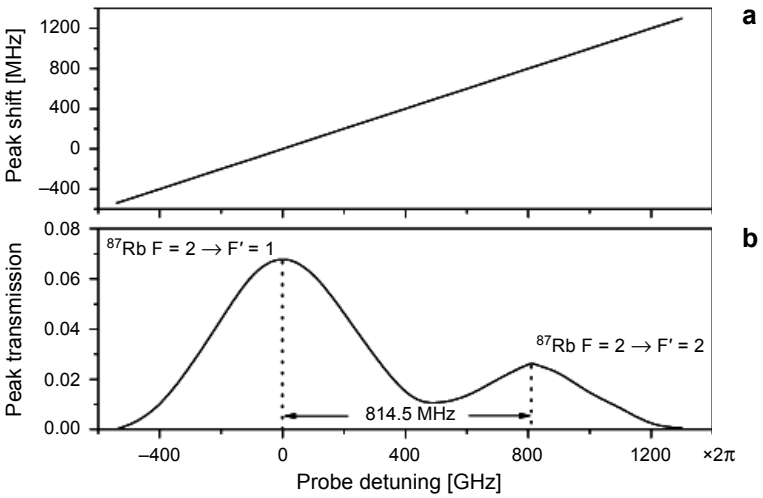

Fig. 6. The dependence of peak shift (**a**) and peak transmission (**b**) on pump detuning from the ^{87}Rb $5S_{1/2}$ $F = 2 \rightarrow 5P_{1/2}$ $F' = 1$ transition when the pump is copropagating with the probe. Other working parameters are the same as Fig. 5.

with the probe and in Fig. 6 when the pump is copropagating with the probe. It can be seen obviously from Figs. 5 and 6 that the filter's center frequency can be tuned over one Doppler width (~532 MHz at 338 K) by utilizing the pump beam to selectively pump different velocity groups of atoms to participate in the filtering process within the Doppler broadened profile. However, the peak transmission decreases with the increment of pump detuning near the relevant resonant pump transitions (*i.e.*, $5S_{1/2}\,F = 2 \rightarrow 5P_{1/2}\,F' = 1$ or 2 transition) mainly because larger pump detuning means lower pump rate, which weakens the transfer ability of the population. Note that when the pump field is on resonance with $5S_{1/2}\ F = 2 \rightarrow 5P_{1/2}\ F' = 2$ transition ($\Delta_c = 814.5$ MHz), the peak transmission is lower than that when the pump field is resonant with $5S_{1/2}$ $F = 2 \rightarrow 5P_{1/2}\ F' = 1$ transition ($\Delta_c = 0$). That is because the hyperfine dipole matrix element for σ^- probe transition $F = 2\ m_F = +2$ to $F' = 2\ m'_F = +1$ ($-\sqrt{1/6}$ expressed as multiples of $\langle J' = 1/2 \| er \| J = 1/2 \rangle$) is less than that for transition $F = 2\ m_F = +2$ to $F' = 1\ m'_F = +1(\sqrt{1/2})$. In addition, by comparing Fig. 5 with Fig. 6, we find that the filter adopting a counterpropagating pump is able to obtain larger tuning capability from –570 to 1360 MHz than that from –540 to 1300 MHz) using a copropagating pump.

The influence of cell temperature and cell length on peak transmission and bandwidth of the ^{87}Rb ground state LIDALF is shown in Figs. 7 and 8, respectively. From which, it can be seen obviously that the peak transmission increases with the increment of cell temperature or cell length. From the physical interpretation of view, the increase in cell temperature or cell length can provide more gaseous atoms to partake in the filtering process, resulting in the augmentation of transmission.

On the basis of the above analyses, it is found that increasing cell temperature, cell length, pump intensity, and decreasing pump detuning can increase the transmission. The increase in transmission results from employing more atoms to involve in filtering

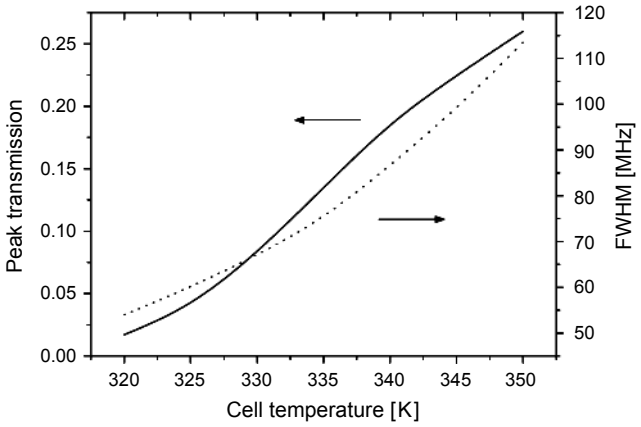

Fig. 7. Peak transmission (solid curve) and FWHM (dotted line) as a function of cell temperature when the pump is counterpropagating with the probe. The pump beam is resonant with ^{87}Rb $5S_{1/2}\ F = 2 \rightarrow 5P_{1/2}\ F' = 1$ transition. The probe beam is on resonance with ^{87}Rb $5S_{1/2}\ F = 2\ m_F = +2 \rightarrow 5P_{1/2}\ F' = 1$ $m'_F = +1$ transition; $I_{\text{pump}} = 40$ mW/cm^2 and $L = 15$ cm.

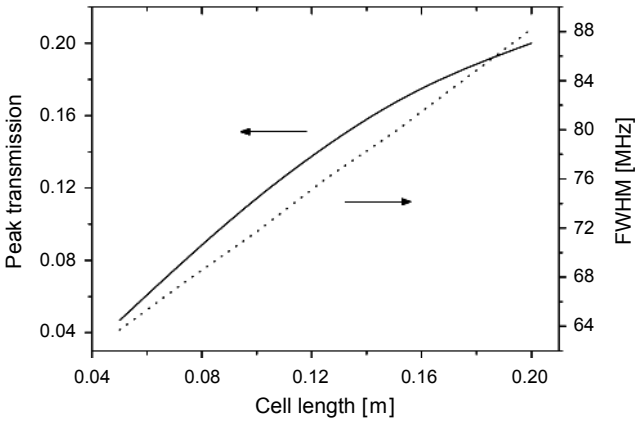

Fig. 8. Peak transmission (solid curve) and FWHM (dotted line) as a function of cell length when the pump is counterpropagating with the probe; $I_{\text{pump}} = 40$ mW/cm^2 and $T = 338$ K. Other working conditions are the same as Fig. 7.

process. Natural rubidium is a mixture of two isotopes, 72.17% ^{85}Rb and 27.83% ^{87}Rb. We can utilize more ^{85}Rb atoms to complete this process in a Rb ground state LIDALF. This Rb filter may be called the ^{85}Rb ground state LIDALF. It operates on the ^{85}Rb $5S_{1/2}\ F = 3 \rightarrow 5P_{1/2}\ F' = 2$ pump transition and $5S_{1/2}\ F = 3\ m_F = +3 \rightarrow 5P_{1/2}\ F' = 2$ $m'_F = +2$ probe transition (Fig. 1). Its pump and probe beams propagate in the opposite direction.

Figure 9 displays the peak transmission and bandwidth of a ^{85}Rb ground state LIDALF as a function of pump intensity at 338 K. As shown in Fig. 9, when the atomic--cell temperature and cell length are constant and pump detuning is zero, the transmission coefficient increases with increasing pump intensity. The increase of transmission

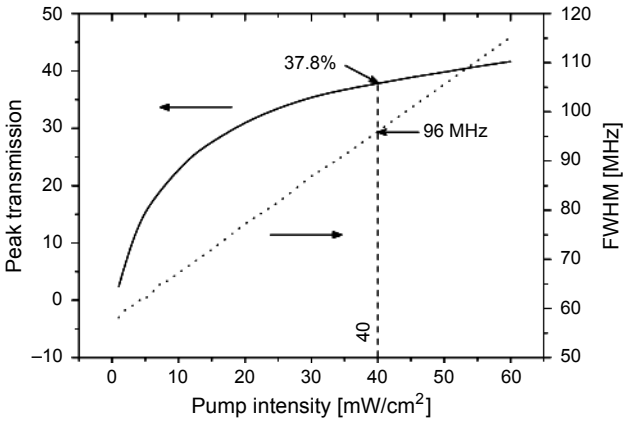

Fig. 9. Peak transmission (solid curve) and FWHM (dotted line) as a function of the pump intensity at 338 K when pump and probe beams are counterpropagating. The pump beam is resonant with ^{85}Rb $5S_{1/2}\ F = 3 \rightarrow 5P_{1/2}\ F' = 2$ transition. The probe beam is on resonance with ^{85}Rb $5S_{1/2}\ F = 3\ m_F = +3 \rightarrow 5P_{1/2}\ F' = 2\ m'_F = +2$ transition; $L = 15$ cm.

becomes slow after the pump intensity increases to a certain value. This kind of phenomena is also shown in Fig. 3, so the same theoretical analysis for it is not presented here. By comparing Fig. 3 with Fig. 9, it is easy to see that at the ^{85}Rb ground state LIDALF it is much easier to obtain a higher peak transmission than at the ^{87}Rb ground state LIDALF in the same working conditions. For example, when pump intensity is 40 mW/cm^2, the peak transmission of the ^{85}Rb ground state LIDALF can reach 37.8%, accompanied by a bandwidth of 96 MHz, while the peak transmission of the ^{87}Rb ground state LIDALF is only 16.8%.

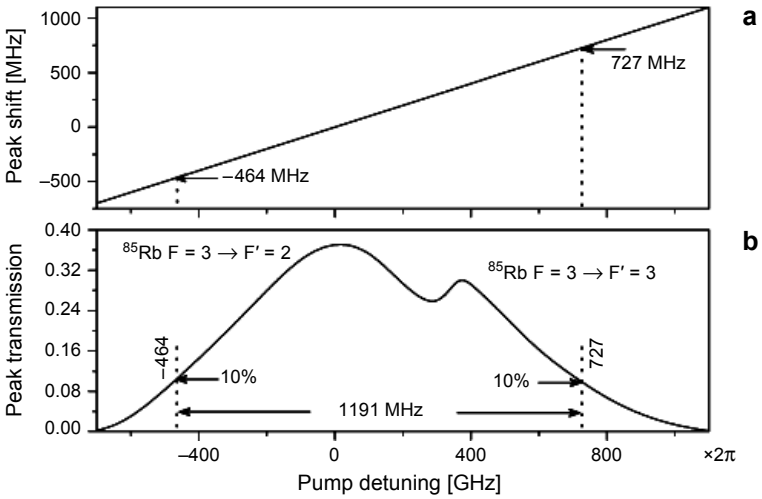

Fig. 10. The dependence of peak shift (**a**) and peak transmission (**b**) on pump detuning from the ^{85}Rb $5S_{1/2}$ $F = 3 \rightarrow 5P_{1/2}$ $F' = 2$ transition when the pump is counterpropagating with the probe; $T = 338$ K, $L = 15$ cm and $I_{\text{pump}} = 40$ mW/cm^2.

The variation of peak transmission and peak shift *vs.* the pump detuning from resonance with ^{85}Rb $5S_{1/2}$ $F = 3 \rightarrow 5P_{1/2}$ $F' = 2$ transition is presented in Fig. 10. From Fig. 10, we find that the ^{85}Rb ground state LIDALF still has a large scale tunability (>1 GHz) under the condition of the peak transmission of above 10%, while the ^{87}Rb ground state LIDALF only obtains a tunability of 482 MHz in the same conditions, as shown in Fig. 5. This result is significant. It means the ^{85}Rb ground state LIDALF can be more effective to achieve a larger tunability than ^{87}Rb ground state LIDALF, which is useful for free-space optical communication and lidar systems subjected to large Doppler shift.

4. Conclusions

In conclusion, we have presented a three-level theoretical model for a ground state atomic optical filter based on velocity-selective optical-pumping-induced dichroism. The influences of pump scheme, pump intensity, pump detuning, cell temperature and cell length on filter's transmission characteristics are analyzed. The results show that

the filter adopting two counterpropagating pump and probe beams has better transmission characteristics, such as higher transmission, narrower bandwidth and larger tunability, than that using two copropagating pump and probe beams. Moreover, the ^{85}Rb ground state LIDALF can be more effective to obtain higher peak transmission and larger tunability than the ^{87}Rb ground state LIDALF, which is important in actual application. The model and analysis presented here are expected to be useful in investigating free-space optical communication, lidar systems and other relevant applications. The model is also suitable for other similar atomic systems.

References

[1] TANG JUNXIONG, WANG QINGJI, LI YIMIN, ZHANG LIANG, GAN JIANHUA, DUAN MINGHAO, KONG JIANKUN, ZHENG LEMIN, *Experimental study of a model digital space optical communication system with new quantum devices*, Applied Optics **34**(15), 1995, pp. 2619–2622.

[2] SHAN XIN, SUN XIANPING, LUO JUN, TAN ZHENG, ZHAN MINGSHENG, *Free-space quantum key distribution with Rb vapor filters*, Applied Physics Letters **89**(19), 2006, article 191121.

[3] POPESCU A., WALLDORF D., SCHORSTEIN K., WALTHER T., *On an excited state Faraday anomalous dispersion optical filter at moderate pump powers for a Brillouin-lidar receiver system*, Optics Communications **264**(2), 2006, pp. 475–481.

[4] ÖHMAN Y., *On some new auxiliary instruments in astrophysical research. VI. A tentative monochromator for solar work based on the principle of selective magnetic ratation*, Stockholms Observatoriums Annaler **19**(4), 1956, pp. 9–11.

[5] YEH P., *Dispersive magnetooptic filters*, Applied Optics **21**(11), 1982, pp. 2069–2075.

[6] YIN B., SHAY T.M., *Theoretical model for a Faraday anomalous dispersion optical filter*, Optics Letters **16**(20), 1991, pp. 1617–1619.

[7] DICK D.J., SHAY T.M., *Ultrahigh-noise rejection optical filter*, Optics Letters **16**(11), 1991, pp. 867–869.

[8] ZHILIN HU, XIANPING SUN, YIPING LIU, LIPING FU, XIZHI ZENG, *Temperature properties of Na dispersive Faraday optical filter at D_1 and D_2 line*, Optics Communications **156**(4–6), 1998, pp. 289–293

[9] CHEN H., SEARCY P., KOREVAAR E., SHE C.Y., *Sodium-vapor dispersive Faraday filter*, Optics Letters **18**(12), 1993, pp. 1019–1021.

[10] YUNDONG ZHANG, XIAOLING JIA, ZUGUANG MA, QI WANG, *Potassium Faraday optical filter in line--center operation*, Optics Communications **194**(1–3), 2001, pp. 147–150.

[11] YUNDONG ZHANG, XIAOLING JIA, ZUGUANG MA, QI WANG, *Optical filtering characteristic of potassium Faraday optical filter*, IEEE Journal of Quantum Electronics **37**(3), 2001, pp. 372–375.

[12] PENG YU-FENG, TANG JUN-XIONG, WANG QING-JI, *Study of Faraday anomalous dispersion spectra of the hyperfine structure of Rb D_2 lines*, Acta Physica Sinica (Overseas Edition) **2**(1), 1993, pp. 1–8.

[13] MENDERS J., BENSON K., BLOOM S.H., LIU C.S., KOREVAAR E., *Ultranarrow line filtering using a Cs Faraday filter at 852 nm*, Optics Letters **16**(11), 1991, pp. 846–848.

[14] BILLMERS R.I., ALLOCCA D.M., GAYEN S.K., SQUICCIARINI M.F., CONTARINO V.M., SCHARPF W.J., *Experimental demonstration of an excited-state Faraday filter operating at 532 nm*, Optics Letters **20**(1), 1995, pp. 106–108.

[15] LIANG ZHANG, JUNXIONG TANG, *Experimental study on optimization of the working conditions of excited state Faraday filter*, Optics Communications **152**(4–6), 1998, pp. 275–279.

[16] TURNER L.D., KARAGANOV V., TEUBNER P.J.O., SCHOLTEN R.E., *Sub-Doppler bandwidth atomic optical filter*, Optics Letters **27**(7), 2002, pp. 500–502.

[17] HE ZHUSONG, ZHANG YUNDONG, LIU SHUANGQIANG, YUAN PING, *Transmission characteristics of an excited-state induced dispersion optical filter of rubidium at 775.9 nm*, Chinese Optics Letters **5**(5), 2007, pp. 252–254.

[18] CERÈ A., PARIGI V., ABAD M., WOLFGRAMM F., PREDOJEVIC A., MITCHELL M.W., *Narrowband tunable filter based on velocity-selective optical pumping in an atomic vapor*, Optics Letters **34**(7), 2009, pp. 1012–1014.

[19] SHUANGQIANG LIU, YUNDONG ZHANG, HAO WU, PING YUAN, *Ultra-narrow bandwidth atomic filter based on optical-pumping-induced dichroism realized by selectively saturated absorption*, Optics Communications **285**(6), 2012, pp. 1181–1184.

[20] SUOMINEN K.-A., STENHOLM S., STÅHLBERG B., *Laser-induced dispersion in a three-level system*, Journal of the Optical Society of America B **8**(9), 1991, pp. 1899–1906.

[21] YUFENG PENG, WENJIN ZHANG, LIANG ZHANG, JUNXIONG TANG, *Analyses of transmission characteristics of Rb, ^{85}Rb and ^{87}Rb Faraday optical filters at 532 nm*, Optics Communications **282**(2), 2009, pp. 236–241.

Received April 25, 2013